ORGANOMETALLICS
Article

Organometallics **2010,** *29,* 6493–6502 6493
DOI: 10.1021/om100832z

Dirhodium Complexes Bridged by Bis(diphenylphosphino)phthalazine ($PNNP^{Ph}$): Central Ring Size and Charge Effects As Compared with the Pyrazolate Derivative ($PNNP^{Py}$)

Takafumi Yamaguchi, Takashi Koike, and Munetaka Akita*

Chemical Resources Laboratory, Tokyo Institute of Technology, R1-27, 4259 Nagatsuta, Midori-ku, Yokohama 226-8503, Japan

Received August 30, 2010

A dirhodium carbonyl complex with 1,4-bis((diphenylphosphino)methyl)phthalazine ($PNNP^{Ph}$), $[(\mu\text{-}\kappa^2\text{:}\kappa^2\text{-}PNNP^{Ph})\{Rh(CO)\}_2](BF_4)_2$, has been prepared and its reactivity studied as compared with the previously reported 3,5-bis((diphenylphosphino)methyl)pyrazolate ($PNNP^{Py}$) analogue $[(\mu\text{-}\kappa^2\text{:}\kappa^2\text{-}PNNP^{Py})\{Rh(CO)_2\}_2]BF_4$. The two quadridentate ligands are different in the size of the central ring and the charge; six-membered ring/neutral ($PNNP^{Ph}$) vs five-membered ring/mononegative ($PNNP^{Py}$). The reactivities of the two systems turn out to be very similar, as can be seen from formation of the analogous, unique tetranuclear μ_4-acetylide ($[(\mu\text{-}PNNP^{Ph})_2\{Rh(CO)\}_4(\mu_4\text{-}C{\equiv}C\text{-}p\text{-}tol)]BF_4$) and μ_4-dicarbide complexes ($[(\mu\text{-}PNNP^{Ph})_2\{Rh(CO)\}_4(\mu_4\text{-}C_2)](BF_4)_2$). However, the $PNNP^{Ph}$ system exhibits the following features. (1) The enlargement of the central ring causes shortening of the metal−metal distance, frequently leading to bond formation between them. For more positively charged $PNNP^{Ph}$ species, (2) back-donation decreases to facilitate CO dissociation and (3) the rhodium centers become more Lewis acidic. Another feature is that the $PNNP^{Ph}$ complex undergoes oxidative addition upon treatment with internal alkynes to form stable adducts with unique coordination structures (e.g., 1,4-dimetallacyclohexa-2,5-diene).

Introduction

Polynuclear species are expected to display unique chemical behavior arising from cooperation of the plural metal centers.[1] Our attention has been focused on the quadridentate, dinucleating 3,5-bis((diphenylphosphino)methyl)pyrazolate ($PNNP^{Py}$) ligand system, which would provide a cis-divacant coordination site effective for cooperative activation of substrates (e.g., **D** in Scheme 1). The synthesis and a preliminary reactivity study of the dirhodium carbonyl adduct $[(\mu\text{-}\kappa^2\text{:}\kappa^2\text{-}PNNP^{Py})\{Rh(CO)_2\}_2]BF_4$ (**C**) were reported by Bosnich in 1985,[2] and recently, we revealed the unique reactivity of **C**: in particular, the formation of tetranuclear species (see Scheme 1).[3] It has been revealed that the inner CO ligands in **C** are so labile owing to the influence of the P donors trans to CO as well as steric reasons that the dicarbonyl species **D** with a cis-divacant site resulting from decarbonylation of **C** serves as an efficient 4e acceptor.[2a,3]

As an extension, we have designed the phthalazine analogue $PNNP^{Ph}$, having the six-membered pyridazine skeleton in place of the five-membered pyrazole ring in the $PNNP^{Py}$ ligand (Scheme 1). The enlargement of the ring part should cause shortening of the distance between the metal centers ($l_1 > l_2$) and, as a result, the $PNNP^{Ph}$ system should have more chances to form a metal−metal bond between the metal centers within the $(\mu\text{-}PNNP^{Ph})Rh_2$ unit (*intraunit*). For the $PNNP^{Py}$ system, no *intraunit* metal−metal bond formation is observed, although cluster species are formed by *interunit* metal−metal bond formation (e.g., **F**). Furthermore, the change of the ring also causes a change in the charge of the ligands. $PNNP^{Py}$ is a mononegative ligand, while $PNNP^{Ph}$ is a neutral one. Such a change should influence the chemical reactivity of the resultant metal complexes.

For the sake of comparison, typical reactions of the $(\mu\text{-}PNNP^{Py})Rh_2$ system are summarized in Scheme 1. The ligand **A**-H is readily converted to the dirhodium cod complex **B** upon treatment with $[Rh(cod)_2]^+/NEt_3$.[2a] Carbonylation of **B** affords the tetracarbonyl complex **C**, which serves as an equivalent to the putative 4e acceptor **D**, upon subsequent in situ decarbonylation.

*To whom correspondence should be addressed. E-mail: makita@res.titech.ac.jp.

(1) Klingele, J.; Dechert, S.; Meyer, F. *Coord. Chem. Rev.* **2009**, *253*, 2698. Braunstein, P.; Oro, L. A.; Raithby, P. R. *Metal Clusters in Chemistry*; Wiley-VCH: Weinheim, Germany, 1999 (3 vols.). Dyson, P. J.; McIndoe, J. S. *Transition Metal Carbonyl Cluster Chemistry*; Gordon and Breach Science: Amsterdam, 2000. Shriver, D. F.; Kaesz, H. D.; Adams, R. D. *The Chemistry of Metal Cluster Complexes*; VCH: New York, 1990. Abel, E. W.; Stone, F. G. A.; Wilkinson, G. *Comprehensive Organometallic Chemistry II*; Pergamon: Oxford, U.K., 1995; Vols. *3*−*10*. Mingos, D. M. P.; Crabtree, R. H. *Comprehensive Organometallic Chemistry III*; Elsevier: Oxford, U.K., 2007; Vols. *4*−*8*.

(2) (a) Schenk, T. G.; Downs, J. M.; Milne, C. R. C.; Mackenzie, P. B.; Boucher, H.; Whelan, J.; Bosnich, B. *Inorg. Chem.* **1985**, *24*, 2334. (b) Schenk, T. G.; Milne, C. R. C.; Sawyer, J. F.; Bosnich, B. *Inorg. Chem.* **1985**, *24*, 2338. See also (c) Bosnich, B. *Inorg. Chem.* **1999**, *38*, 2554.

(3) (a) Tanaka, S.; Akita, M. *Angew. Chem., Int. Ed.* **2001**, *40*, 2865. (b) Tanaka, S.; Dubs, C.; Inagaki, A.; Akita, M. *Organometallics* **2004**, *23*, 317. (c) Dubs, C.; Inagaki, A.; Akita, M. *Chem. Commun.* **2004**, 2760. (d) Tanaka, S.; Dubs, C.; Inagaki, A.; Akita, M. *Organometallics* **2005**, *24*, 163. (e) Dubs, C.; Yamamoto, T.; Inagaki, A.; Akita, M. *Organometallics* **2006**, *25*, 1344. (f) Dubs, C.; Yamamoto, T.; Inagaki, A.; Akita, M. *Organometallics* **2006**, *25*, 1359. (g) Dubs, C.; Yamamoto, T.; Inagaki, A.; Akita, M. *Chem. Commun* **2006**, 1962.

Published on Web 11/03/2010

Scheme 1

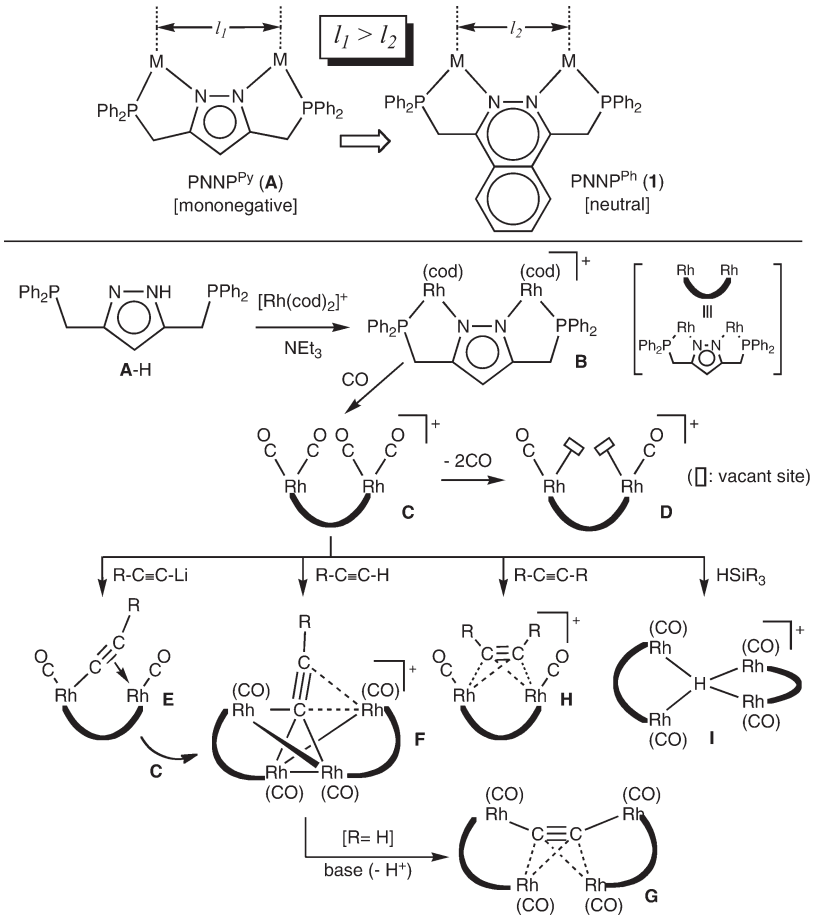

Scheme 2

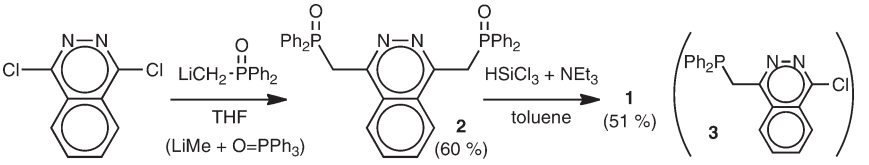

Treatment of **C** with lithium acetylide provides the dinuclear μ-η^1:η^2-acetylide **E**, which is further converted to the tetranuclear μ_4-acetylide **F** by treatment with **C**.[3b,d] The tetranuclear complex **F** has been directly obtained from terminal alkyne upon treatment with **C**. Interestingly, the tetranuclear μ_4-C≡CH complex (**F**; R = H) is converted to the μ_4-dicarbide complex **G** by deprotonation.[3b,d] The complexes **E**−**G** show fluxional behavior, and it is notable that the mechanisms for the fluxional behavior of **F** and **G** involve reversible metal−metal bond cleavage and recombination processes. Reaction of **C** with internal alkyne forms the unstable μ-η^2:η^2 adduct **H**.[3d] In contrast to the incorporation of acetylide and alkyne (4e donors), the unique μ_4-hydride complex **I** is formed by reaction of **C** with hydrosilane.[3b,d]

Herein we disclose (1) the synthesis of the PNNP^{Ph} ligand and its group 9 metal complexes and (2) reactions of the resultant dirhodium carbonyl species toward alkynes and $HSiEt_3$, furnishing unique adducts.

Results and Discussion

Ligand Synthesis. We designed a synthetic route to the PNNP^{Ph} ligand **1** following the relevant hexadentate N_6 ligand with the phthalazine core developed by Lippard (Scheme 2).[4] Ligand **1** was readily prepared by a two-step process: (1) overnight reaction of 1,4-dichlorophthalazine with an excess amount of $LiCH_2P(=O)Ph_2$ (generated by treatment of $O=PPh_3$ with MeLi)[5] followed by (2) reduction of the resultant phosphine oxide derivative **2** with $HSiCl_3/NEt_3$. A shorter reaction time or a smaller amount of the lithium reagent caused formation of the monosubstituted product **3**. Ligand **1** could not be obtained by direct substitution reaction of 1,4-dichlorophthalazine with $LiCH_2PPh_2$.[6] Ligand **1** is readily characterized on the basis of its spectroscopic data (δ_P −18.7; for other data, see the Experimental Section), which supports the symmetrical structure.

Preparation of COD Complexes. Reaction of the obtained PNNP^{Ph} ligand **1** with labile cod complexes of rhodium and iridium, $[M(cod)_2]BF_4$, afforded the dicationic 1:2 adducts **4**, $[(\mu\text{-}\kappa^2\text{:}\kappa^2\text{-PNNP}^{Ph})\{M(cod)\}_2](BF_4)_2$, as yellow (**4a**) and red

(4) Barrios, A. M.; Lippard, S. J. *J. Am. Chem. Soc.* **1999**, *121*, 11751.
(5) Seyferth, D.; Welch, D. E.; Heeren, J. K. *J. Am. Chem. Soc.* **1964**, *86*, 1100.
(6) Peterson, D. J. *J. Organomet. Chem.* **1967**, *8*, 199.

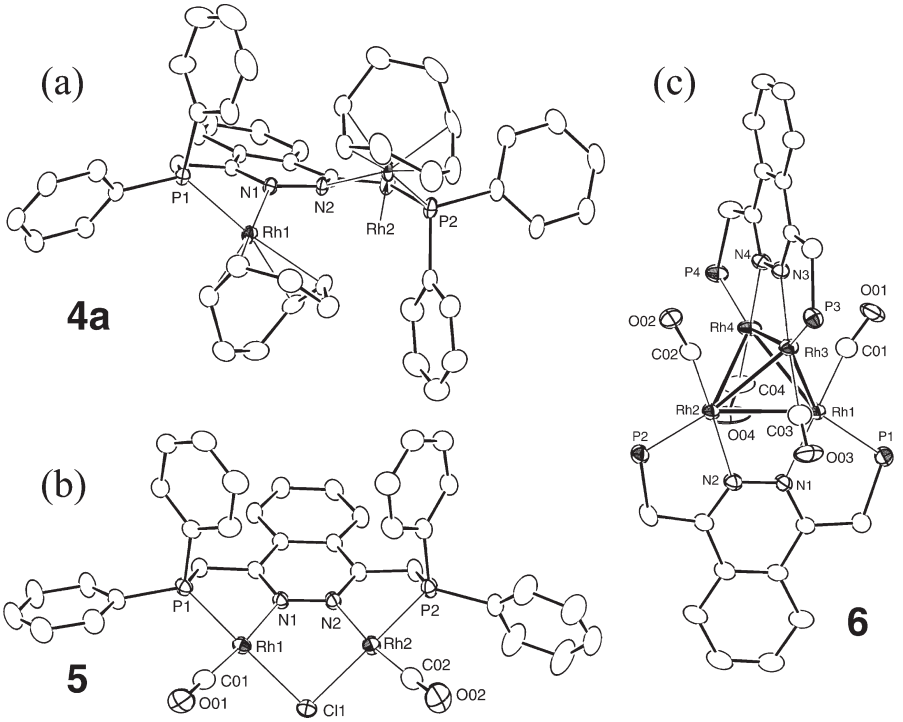

Figure 1. ORTEP views of the cationic parts of **4a** (a), **5** (b), and **6** (c) with thermal ellipsoids at the 30% probability level. For **6**, phenyl groups are omitted for clarity.

Scheme 3

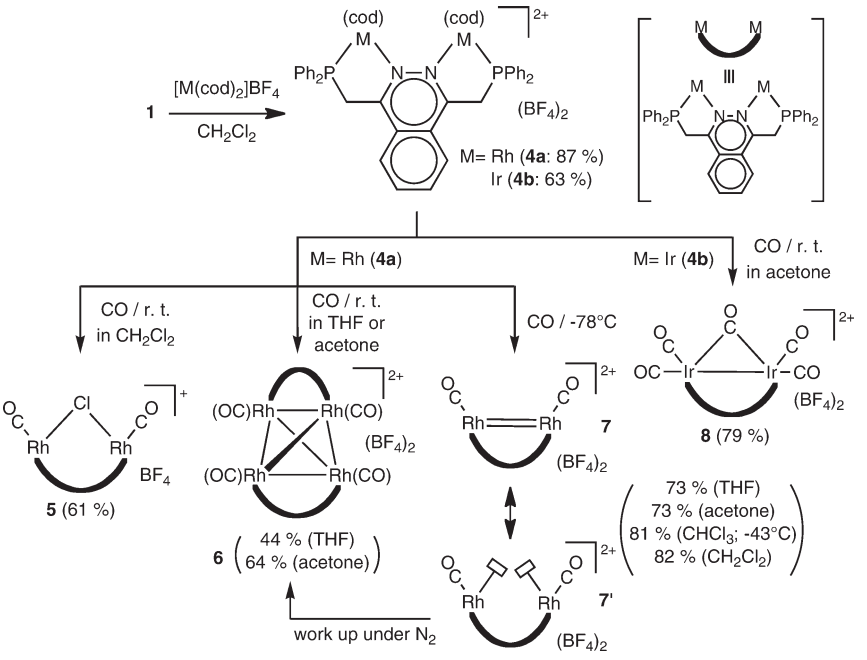

crystals (**4b**), respectively (Scheme 3). The composition and symmetrical structure of the products are confirmed by the single sets of NMR signals for the phthalazine, CH_2P, and cod parts, and P coordination is verified for **4a** by the doublet ^{31}P NMR signal (δ_P 28.0 (d, J_{P-Rh} = 148.4 Hz)) resulting from coupling with the Rh nucleus.

The two cod complexes have also been characterized by X-ray crystallography (Figure 1a; for **4b**, see the Supporting Information), which reveals (1) square-planar geometry of the metal centers coordinated by the bridging μ-κ^2:κ^2-PNNP^{Ph} ligand and the η^2:η^2-cod ligand, (2) twisting of the structure with respect to the N1−N2 bond (<M1−N1−N2−M2 = 53.3(4)° (**4a**), 52(1)° (**4b**)) caused by the bulky M(cod) fragments, and (3) M···M separations (3.949(2) Å (**4a**), 3.928(2) Å (**4b**)) substantially longer than the sum of covalent radii (Rh, 2.68 Å; Ir, 2.71 Å).

Carbonylation of COD Complexes. In the case of the PNNP^{Py} system carbonylation of the cod complex **B** in CH_2Cl_2 afforded the simply substituted tetracarbonyl complex **C**, without a Rh−Rh bond (Scheme 1).[2a] Carbonylation

Table 1. Structural Parameters for Tetrahedral Tetrarhodium Complexes 6 and 10

	6	10
	Bond Lengths (Å)	
Rh1−Rh2	2.9410(9)	2.860(1)
Rh1−Rh3	2.814(1)	2.9977(9)
Rh1−Rh4	2.8558(9)	2.7182(9)
Rh2−Rh3	2.875(1)	2.755(1)
Rh2−Rh4	2.8614(9)	2.881(1)
Rh3−Rh4	2.905(1)	2.926(1)
Rh−P	2.241(2)−2.251(2)	2.248(2)−2.289(3)
Rh−N	2.065(5)−2.073(5)	2.035(8)−2.145(7)
	1.855(9) (Rh1−C1)	2.00(1) (C11−Rh1)
	1.854(7) (Rh2−C2)	1.20(2) (C11−C12)
	1.849(8) (Rh3−C3)	2.01(1) (C21−Rh3)
	1.824(8) (Rh4−C4)	1.21(1) (C21−C22)
	Bond Angles (deg)	
	168.2(7) (Rh1−C1−O1)	172.0(8) (Rh1−C11−C12)
	169.8(7) (Rh2−C2−O2)	170(1) (C11−C12−C13)
	168.0(8) (Rh3−C3−O3)	171.5(9) (Rh3−C21−C22)
	169.7(9) (Rh4−C4−O4)	172(1) (C21−C22−C23)

of the $PNNP^{Ph}$ complex **4a** in CH_2Cl_2 in a manner analogous to that of **B** (Scheme 2) gave the carbonylated μ-Cl complex **5** (Figure 1b; Rh1···Rh2 = 3.42873(3) Å) resulting from carbonylation as well as Cl abstraction from the solvent. Similar Cl abstraction was also observed for the $PNNP^{Py}$ system but was much slower than that of the $PNNP^{Ph}$ system.

Then carbonylation was carried out in non-halogenated solvents such as THF and acetone. The obtained product was not a monomeric dinuclear species but a dimeric tetranuclear species with a tetrahedral Rh_4 core, $[(\mu\text{-}PNNP^{Ph})_2\{Rh(CO)\}_4](BF_4)_2$ (**6**), as revealed by X-ray crystallography (Figure 1c and Table 1). The Rh−Rh distances of ca. 2.8−2.9 Å in **6** are at the longer end of bonding interactions and are substantially longer than those in the related cluster compound $Rh_4(CO)_{12}$ (~2.7 Å).[7] It is notable that complex **6** contains *intraunit* Rh−Rh bonds, in contrast to the $PNNP^{Py}$ system. The distances of the Rh−Rh bonds bridged by the $PNNP^{Ph}$ ligand (~2.9 Å) are slightly longer than those not supported by the ligand (~2.8 Å). These structural features suggest that the coordinative unsaturation is delocalized over the Rh_4 core with an average Rh−Rh bond order of 7/6. The tetrarhodium species **6** is a coordinatively unsaturated species with 58 cluster valence electrons (CVE) (cf. 60 CVE for a coordinatively saturated species). According to the Cambridge Structural Database (CSD), only two Rh_4 species with 58 CVE have been reported and both of them contain four bridging hydride ligands.[8] No hydride ^1H NMR signal is detected for **6** (up to −30 ppm). Simple dimerization of the dirhodium species **7** (see below) gives a 56-CVE species, and such a highly coordinatively unsaturated species should be stabilized by the 2e reduction to give the 58-CVE species **6**, although the reductant is not clear. The coordination structural change from a 16e square-planar geometry as in **4**, **5**, and **7** to the six-coordinate structure (preferably with an 18e configuration) should be, in part, the cause of the electron deficiency of the tetranuclear species, including those discussed below.

(7) Wei, C. H. *Inorg. Chem.* **1969**, *8*, 2384. Farrugia, L. J. *J. Cluster Sci.* **2000**, *11*, 39.

(8) Kulzick, M.; Price, R. T.; Muetterties, E. L.; Day, V. W. *Organometallics* **1982**, *1*, 1256. (b) Espinet, P.; Bailey, P. M.; Piraino, P.; Maitlis, P. M. *Inorg. Chem.* **1979**, *18*, 2706.

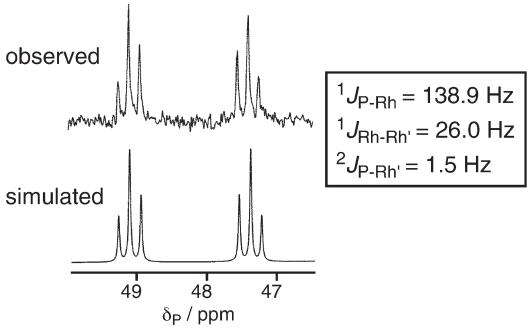

Figure 2. Observed and simulated ^{31}P NMR spectra of **7** (observed in CD_3NO_2 at 81 MHz at room temperature).

Carbonylation of **4a** at −78 °C followed by precipitation by addition of hexane at the same temperature afforded the dicarbonyl species **7** as a yellow solid. Complex **7** was also obtained even in chlorinated solvents, when carbonylation was carried out at low temperatures. The product **7** was unstable in the absence of CO. When workup of the reaction mixture for the carbonylation of **4a** was carried out under an N_2 atmosphere, the Rh_4 species **6** was obtained instead of **7**. While the instability of **7** hampered its thorough characterization, the spectroscopic analysis described below led to characterization of **7** as the dirhodium dicarbonyl species shown in Scheme 3. The ^1H NMR spectrum of **7** contains single sets of the phthalazine and CH_2 signals, suggesting a symmetrical structure, and its IR spectrum contains a single CO vibration at 2045 cm^{-1}. These data are consistent with the formulation of the product as $[(\mu\text{-}\kappa^2\text{:}\kappa^2\text{-}PNNP^{Ph})\{Rh(CO)\}_2]BF_4$. Crucial information has been obtained from a ^{31}P NMR spectrum, which contains a doublet-of-triplets-like signal (Figure 2), in sharp contrast to the simple doublet signal observed for the cod (**4a**) and μ-Cl complexes (**5**). Simulation analysis reveals that the spectrum is best reproduced by taking into account three spin−spin couplings, $^1J_{RhP}$, $^1J_{RhRh'}$, and $^2J_{RhP'}$, as compared in Figure 2. The last two couplings verify bonding interactions between the two rhodium centers, and such coupling is not observed for complexes without a Rh−Rh interaction (e.g., **4** and **5**).[9] On the basis of these data, the dicarbonyl species **7** has been assigned to the dinuclear species with a Rh═Rh bond as shown in Scheme 3,[10] which is in resonance with the coordinatively unsaturated structure **7′**, analogous to **D**. The reactivity of **7** toward alkynes described below is also consistent with the formulation as a 4e acceptor. In the following experiments the unstable species **7** was generated from **4a** under a CO atmosphere at −78 °C and used without isolation at the same temperature because of its instability.

(9) The J_{RhRh} coupling is a useful diagnostic for a Rh−Rh bonding interaction. Rh−Rh-bonded species such as **6** and **7** do not always show a sharp doublet ^{31}P NMR signal due to $^1J_{RhRh}$ and/or $^2J_{RhP}$ coupling. Simulation analysis is not always successful, and in such cases, the ^{31}P NMR signals are denoted as multiplet signals in this paper. A very small $^2J_{RhP}$ or $^3J_{PP}$ coupling (< 3 Hz) is also observed, even for non-Rh−Rh-bonded species such as **9** and **13** having μ-C≡CR and μ-OH ligands, respectively.

(10) Complex **7** was also examined by VT ^{13}C NMR measurements of a ^{13}CO-enriched sample. A broad singlet signal observed at room temperature (δ_C 184 (in CD_2Cl_2)) separated into several signals below −60 °C (δ_C ~181 (br), 183.6, 184.0, 184.4, ~210 (br)). The complicated behavior should be ascribed to a CO coordination/dissociation equilibrium. Because complex **7** decomposed in the absence of CO, however, we could not obtain a ^{13}C NMR spectrum of **7** in the absence of CO.

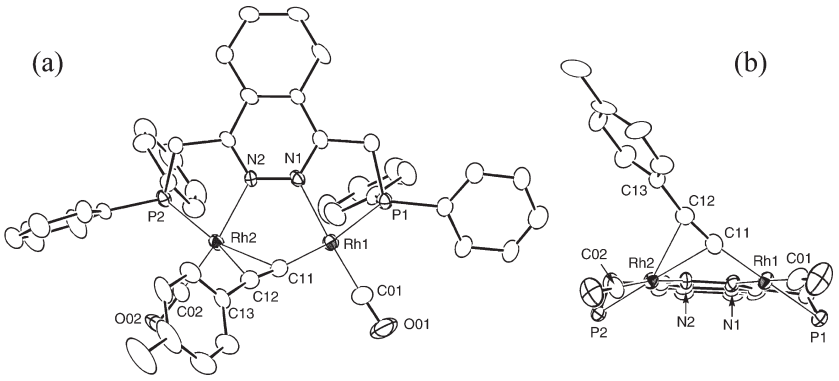

Figure 3. ORTEP views of the cationic part of **9** drawn with thermal ellipsoids at the 30% probability level: (a) top view; (b) side view of the core part.

Scheme 4

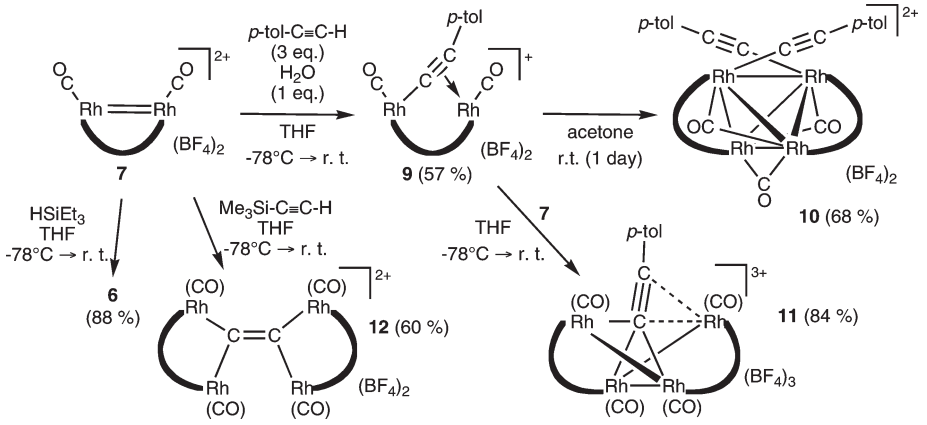

Carbonylation of the iridium analogue **4b** resulted in the formation of the pentacarbonyldiiridium complex **8**, which was characterized on the basis of spectroscopic and preliminary crystallographic data. The carbonyl complex **8** turned out to be a coordnatively saturated 34e species with a metal−metal single bond and a bridging CO ligand ($\nu(\mu$-CO) 1751 cm^{-1}), which is totally different from the structures of the rhodium analogues **5**−**7**.

Reaction of Rhodium CO Complex 7 with $HSiEt_3$ and Alkynes. The labile rhodium carbonyl species **7** was treated with hydrosilane and alkynes, which reacted with the $PNNP^{Py}$ analogue **C** to afford unique di- and tetranuclear complexes (Scheme 1).[3]

(i). With $HSiEt_3$. In contrast to the reaction of the $PNNP^{Py}$ complex **C** with hydrosilane, giving the tetranuclear μ_4-hydride complex **I** (Scheme 1),[3a,d] the analogous reaction of **7** with $HSiEt_3$ gave the tetrarhodium complex **6** without the hydride ligand (Scheme 4). The reaction may initially form a hydride species, $[(\mu\text{-}PNNP^{Ph})Rh_2(CO)_2(\mu\text{-}H)]^+$, which couples with a second molecule of **7** to form a tetrarhodium μ-hydride intermediate analogous to **I**, $[(\mu\text{-}PNNP^{Ph})_2Rh_4(CO)_4(\mu_x\text{-}H)]^{3+}$. The resultant +3 species, however, is so acidic that it may undergo deprotonation to form the non-hydride tetrarhodium cluster compound **6** with +2 charge.

(ii). With Terminal Alkyne. Reaction of the $PNNP^{Ph}$ species **7** with terminal alkyne was dependent on the reaction conditions, and core parts of some of the reaction products turned out to be isostructural with those of the $PNNP^{Py}$ derivatives.

Reaction of the carbonyl species **7** or the μ-Cl complex **5** with a lithium acetylide, LiC≡C-*p*-tol, gave a mixture of products, in contrast to the clean reaction of the $PNNP^{Py}$ system. Direct reaction of **7** with HC≡C-*p*-tol in the presence of water afforded the dirhodium μ-η^1:η^2-acetylide complex **9** (Scheme 4), analogous to the $PNNP^{Py}$ derivative **E** (Scheme 1), whereas the reaction in the absence of water gave an unidentified product.[11] In contrast, complex **9** has been characterized by spectroscopic data and, as usually observed for the related complexes, it shows fluxional behavior by way of a windshield wiper like motion, which leads to mirror-symmetrical NMR features for the $(\mu\text{-}PNNP^{Ph})Rh_2$ moiety at room temperature.[12] Complex **9** was also characterized by X-ray crystallography (Figure 3 and Table 2) and is a good sample for comparison of the structural features of the two PNNP ligand systems. For the $(\mu\text{-L})Rh_2(CO)_2$ part, first of all, the Rh···Rh separation in **9** is shorter than that in **E** (R = *p*-tol) by ca. 0.27 Å, as we expected. The Rh−N distances of **9** are slightly shortened compared to those of **E** (R = *p*-tol), presumably reflecting the different charges of L ($PNNP^{Py}$ negative vs $PNNP^{Ph}$ neutral), whereas the Rh−P distances are comparable. On the other hand, no

(11) The unidentified product presumably contains a Rh-C(=O)C(*p*-tol)=C(H)-C(=O) fragment like that found in **13** and a μ-acetylide functional group like that in **9**.

(12) VT measurements (~-90 °C) were carried out for the fluxional complexes, but a spectrum at the slow exchange limit was not obtained, although broadening of the spectra was observed for some of the complexes.

Table 2. Comparison of Structural Parameters for the Dirhodium μ-*p*-Tolylacetylide Complexes [(μ-L){Rh(CO)}$_2$(μ-C≡C-*p*-tol)](BF$_4$)$_n$ (L/n = PNNP^{Ph}/1 (9**), PNNP^{Py}/0 (**E** (R = *p*-tol))[a]**

	9	**E** (R = *p*-tol)[b]
	Bond Lengths (Å)	
Rh1···Rh2	3.341(1)	3.6169(4)
Rh1−P1	2.270(3)	2.2768(8)
Rh1−N1	2.106(7)	2.030(2)
Rh1−C01	1.81(1)	1.826(3)
Rh2−P2	2.226(3)	2.2405(7)
Rh2−N2	2.119(7)	2.066(2)
Rh2−C02	1.80(1)	1.825(3)
C11−Rh1	2.00(1)	2.061(3)
C11−Rh2	2.25(1)	2.338(2)
C12−Rh2	2.39(1)	2.388(3)
C11−C12	1.23(2)	1.205(5)
C12−C13	1.46(2)	1.448(5)
	Bond Angles (deg)	
P1−Rh1−N1	80.2(2)	80.07(8)
P1−Rh1−C01	96.6(4)	99.1(1)
N1−Rh1−C11	90.3(4)	88.2(1)
C01−Rh1−C11	92.9(5)	92.7(1)
P2−Rh2−N2	79.9(2)	77.89(6)
P2−Rh2−C02	90.9(4)	93.15(9)
N2−Rh2−C11	84.7(3)	82.55(9)
C02−Rh2−C11	104.7(4)	105.22(9)
Rh1−C11−Rh2	103.6(4)	110.5(1)
Rh1−C11−C12	169.7(8)	168.7(3)
Rh2−C11−C12	80.8(7)	77.5(2)
Rh2−C12−C11	68.6(7)	73.0(2)
C11−C12−C13	169(1)	164.3(3)

[a] A unit cell of **9** contains two independent molecules with essentially the same geometry, and the parameters for one of them are shown. [b] References 3b,3d.

significant differences are noted for the Rh$_2$(μ-C≡C) part. This would result from the fact that the strain of the Rh$_2$(μ-C≡C) part can be released by twisting the square-planar Rh coordination planes, as can be seen from a side view (Figure 3b). The five-membered Rh−N−C−C−P ring adopts an envelope-like conformation by puckering of the Rh−P−C moieties.

The notable effect of water suggests the following formation mechanism of **9**: coordination of water to **7** followed by deprotonation forms the μ-hydroxo intermediate [(μ-PNNP^{Ph})-{Rh(CO)}$_2$(μ-OH)]$^+$, which undergoes dehydrative condensation with terminal alkyne to produce **9**. Similar deprotonation occurs for the PNNP^{Py} system during the formation of the tetranuclear species **F** from the carbonyl precursor **C**.[3c,d] In contrast to the PNNP^{Py} system (**C** → **F**), the tetranuclear μ_4-acetylide cluster compound **11**, like **F**, cannot be obtained directly from **8** by a one-pot reaction but by another method (see below).

The dinuclear μ-acetylide complex **9** was not so stable as to be gradually converted to the tetranuclear diacetylide cluster complex **10** via decarbonylation associated with dimerization of the Rh$_2$(μ-C≡CR) core of **9**. X-ray crystallography of **10** reveals the presence of a tetrahedral Rh$_4$ core with Rh−Rh distances between 2.7182(9) and 2.9977(9) Å (Figure 4a and Table 1). The Rh−Rh bonds, except the Rh1−Rh3 bond, are associated with the bridging ligands (PNNP^{Ph} or CO), and accordingly, the Rh1−Rh3 bond (2.9977(9) Å) is the longest among them. The two acetylide groups are σ-bonded to the rhodium centers, as indicated by no apparent π interaction with the neighboring rhodium centers (2.517(9) (C11−Rh3), 2.640(9) Å (C11−Rh4), 2.579(9) Å (C21−Rh1), 2.53(1) Å (C21−Rh2)) as well as the linear Rh−C≡C linkages (172.0(8)° (Rh1−C11−C12), 171.5(9)° (Rh3−C21−C22)). This is a rare example of a σ-bonded acetylide cluster compound without π interaction.[13] Taking into account the electron-deficient configuration of the Rh$_4$ cores with 58 CVE, 2e short of a saturated configuration (60 CVE), it should be noted that the cluster part remains coordinatively unsaturated even in the presence of the π donor (acetylide) in the vicinity. Decarbonylation of **9** forms a coordinatively unsaturated monocarbonyl intermediate, [(μ-PNNP^{Ph})Rh$_2$(CO)(C≡C-*p*-tol)]$^+$, which captures another molecule of **9** via metal−metal bond formation to furnish **10**.[3b,d]

The tetrarhodium μ_4-acetylide cluster compound **11** was prepared by following a synthetic route analogous to that of **F** (Scheme 1; **E** + **C** → **F**).[3b,d] Simple mixing of equimolar amounts of **9** and **7** in THF at room temperature gave **11** (Scheme 4). The spectroscopic properties of **11**, including fluxional behavior via reversible metal−metal bond cleavage and recombination processes, are very similar to those of **F**;[3b,d,12] single sets of ^{1}H and ^{31}P NMR signals for the CH$_2$P parts are observed. The coordinatively unsaturated species **7** readily couples with **9** to form the tetranuclear adduct **11**. Structural features of **11** (Figure 4b and Table 3) also turn out to be very similar to those of **F**. The acetylide ligand is coordinated to the folded Z-shaped metal array in a μ_4-η^1(Rh1):η^1(Rh3):η^1(Rh4):η^2(Rh2) fashion.

The tetrarhodium μ_4-dicarbide complex **12**,[14,15] analogous to the PNNP^{Py} derivative **G**, was obtained by treatment of **7** with Me$_3$SiC≡CH. In contrast to the PNNP^{Py} system, the μ_4-C$_2$ complex **12** was formed directly, and no μ_4-acetylide intermediate **11** (R = SiMe$_3$, H) analogous to **F** was detected. The molecular structure of the fluxional molecule **12**[12] has been determined by X-ray crystallography (Figure 4c). The C−C distance of 1.24(2) Å is similar to that of **G** (1.249(7) Å), as compared in Table 4, but the coordination structure of the central C$_2$ part is changed from a double μ-η^1:η^2 coordination (μ_4-η^1:η^1:η^2:η^2) (**G**) to a μ_4-η^1:η^1:η^1:η^1 coordination (**12**),[15] as indicated by the significant difference in the distances between the Rh2 atom and the two C$_2$ atoms (0.54 Å (**12**); cf. 0.03−0.04 Å (**G**)). The more η^2 coordination character in **G** is evident

(13) Cherkas, A. A.; Taylor, N. J.; Carty, A. J. *Chem. Commun.* **1990**, 385. Yamagata, T.; Okiyama, H.; Imoto, H.; Saito, T. *Acta Crystallogr., Sect. C* **1997**, *53*, 859. Kizas, O. A.; Krivykh, V. V.; Vorontsov, E. V.; Tok, O. L.; Dolgushin, F. M.; Koridze, A. A. *Organometallics* **2001**, *20*, 4170. Wong, W.-Y.; Ting, F.-L.; Lam, W.-L. *Eur. J. Inorg. Chem.* **2001**, 623. For planar Pt cluster compounds, see: Smith, D. E.; Welch, A. J.; Treurnicht, I.; Puddephatt, R. J. *Inorg. Chem.* **1986**, *25*, 4616. Che, C.-M.; Yip, H.-K.; Lo, W.-C.; Peng, S.-M. *Polyhedron* **1994**, *13*, 887. Leoni, P.; Marchetti, F.; Marchetti, L.; Pasquali, M. *Chem. Commun.* **2003**, 2372. Albinati, A.; de Biani, F. F.; Leoni, P.; Marchetti, L.; Pasquali, M.; Rizzato, S.; Zanello, P. *Angew. Chem., Int. Ed.* **2005**, *44*, 5701. Cavazza, C.; de Biani, F. F.; Funaioli, T.; Leoni, P.; Marchetti, F.; Marchetti, L.; Zanello, P. *Inorg. Chem.* **2009**, *48*, 1385.

(14) Bruce, M. I.; Low, P. J. *Adv. Organomet. Chem.* **2004**, *50*, 180.

(15) μ_4-η^1:η^1:η^1:η^1-C$_2$ complexes: (a) Griffith, C. S.; Koutsantonis, G. A.; Skelton, B. W.; White, A. H. *J. Organomet. Chem.* **2005**, *690*, 3410. (b) Akita, M.; Sugimoto, S.; Tanaka, M.; Moro-oka, Y. *J. Am. Chem. Soc.* **1992**, *114*, 7581. (c) Akita, M.; Sugimoto, S.; Hirakawa, H.; Kato, S.; Terada, M.; Tanaka, M.; Moro-oka, Y. *Organometallics* **2001**, *20*, 1555. (d) Terada, M.; Higashihara, G.; Inagaki, A.; Akita, M. *Chem. Commun.* **2003**, 2984. (e) Terada, M.; Akita, M. *Organometallics* **2003**, *22*, 355. (f) Higashihara, G.; Terada, M.; Inagaki, A.; Akita, M. *Organometallics* **2007**, *26*, 439. Double μ-η^1:η^2-C$_2$ complexes: (g) Bruce, M. I.; Snow, M. R.; Tiekink, E. R. T.; Williams, M. L. *Chem. Commun.* **1986**, 701. (h) Yam, V. W.-W.; Fung, W. K.-M.; Cheung, K.-K. *Angew. Chem., Int. Ed.* **1996**, *35*, 1100. (i) Mihan, S.; Sunkel, K.; Beck, W. *Chem. Eur. J.* **1999**, *5*, 745. (j) Song, H.-B.; Wang, Q.-M.; Zhang, Z.-Z.; Mak, T. C. W. *Chem. Commun.* **2001**, 1658. (k) Hooper, T. N.; Green, M.; Russell, C. A. *Chem. Commun.* **2010**, *46*, 2313.

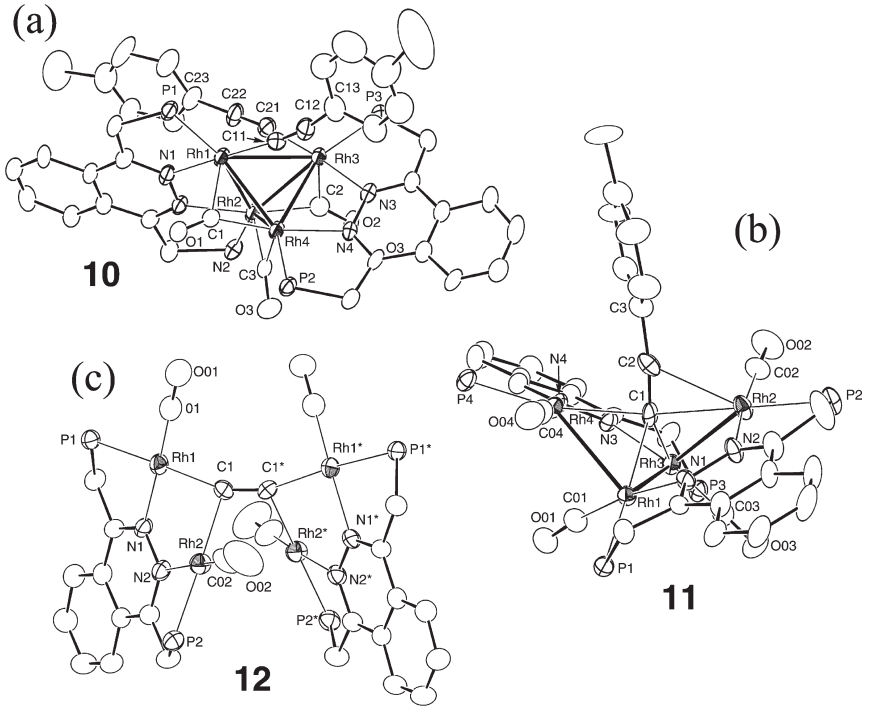

Figure 4. ORTEP views of the cationic parts of **10** (a), **11** (b), and **12** (c) drawn with thermal ellipsoids at the 30% probability level. Phenyl groups are omitted for clarity.

Table 3. Comparison of Structural Parameters (Bond Lengths in Å) for the Tetrarhodium μ_4-*p*-Tolylacetylide Cluster Compounds $[(\mu\text{-L})_2\{Rh(CO)\}_4(\mu\text{-C}\equiv\text{C-}p\text{-tol})](BF_4)_n$ (L/*n* = $PNNP^{Ph}$/3 (11), $PNNP^{Py}$/1 (F (R = *p*-tol))[a]

	11	**F** (R = *p*-tol)[b]
Rh1−Rh3	2.856(1)	2.8925(4)
Rh1−Rh4	2.894(1)	2.9474(5)
Rh2−Rh3	2.967(3)	2.9732(5)
Rh−P	2.211(3)−2.245(2)	2.218(1)−2.264(1)
Rh−N	2.116(8)−2.142(7)	2.042(4)−2.062(4)
C1−Rh1	2.18(1)	2.151(4)
C1−Rh2	2.246(9)	2.309(4)
C1−Rh3	2.17(1)	2.223(4)
C1−Rh4	2.313(9)	2.335(4)
C2−Rh2	2.47(1)	2.386(5)
C2···Rh4	2.55(1)	2.555(5)
C1−C2	1.24(2)	1.249(7)
C2−C3	1.44(2)	1.441(7)

[a] Bond angles (in deg): **11**, Rh3−Rh1−Rh4 = 75.49(3), Rh1−Rh3−Rh2 = 74.54(3), C1−C2−C3 = 173(1); **F**, Rh3−Rh1−Rh4 = 80.13(2), Rh1−Rh3−Rh2 = 77.62(1), C1−C2−C3 = 172.3(5). [b] References 3b,3d.

Table 4. Comparison of Structural Parameters (Bond Lengths in Å) for the Tetrarhodium μ_4-Dicarbide Cluster Compounds $[(\mu\text{-L})_2\{Rh(CO)\}_4(\mu\text{-C}_2)](BF_4)_n$ (L/*n* = $PNNP^{Ph}$/2 (12), $PNNP^{Py}$/0 (G))[a]

	12[b]	**G**[c,d]
Rh1···Rh2	3.1967(9)	3.815(2), 3.849(1)
Rh2···Rh2*	3.009(3)	3.173(2)
Rh1−P1	2.254(2)	2.259(2), 2.258(2)
Rh2−P2	2.234(2)	2.230(4), 2.219(3)
Rh1−N1	2.088(6)	2.03(1), 2.042(9)
Rh2−N2	2.110(6)	2.079(5), 2.069(6)
Rh1−C01	1.82(1)	1.82(2), 1.81(1)
Rh2−C02	1.80(1)	1.83(1), 1.810(8)
C1−C1*	1.23(1)	1.22(1)
C1−Rh1	2.015(6)	2.042(9), 2.062(9)
C1−Rh2	2.195(8)	2.44(2), 2.44(1)
C1*−Rh2	2.737(7)	2.396(9), 2.41(1)

[a] Bond angles (in deg): **12**, Rh1−C1−Rh2 = 98.7(3), Rh1−C1−C1* = 159.0(5), Rh2−C1−C1* = 102.2(4); **G**, Rh1−C1−Rh2 = 116.5(4), 117.2(3), Rh1−C1−C1* = 163.4(7), 164.0(8), Rh2−C1−C1* = 74(1), 73.3(7). [b] Imposed on a crystallographic C_2 axis. [c] With no crystallographic symmetry within the molecule. [d] References 3b,3d.

from the similar Rh−C bond distances. Accordingly, the C_2 carbon atoms become planar, as judged by the sum of the bond angles (359.9° (**12**) vs 353.9, 354.5° (**G**)). However, the $(\mu_4\text{-}C_2)Rh_4$ part still deviates from a D_{2h}-symmetrical, planar tetrametalated ethylene structure, $M_2C{=}CM_2$,[15] as is evident from (1) the unsymmetrical bonding of the C1 atom to the two rhodium centers (C1−Rh1 = 2.015(6) Å, C1−Rh2 = 2.195(8) Å; difference 0.18 Å) and (2) the dihedral angle Rh2−C2−C2*−Rh2* (58.3°). The deviation may result from the following two factors. One is steric repulsion between the bulky metal fragments, as can be seen from the overall molecular structure. The other is intrinsic preference of the $M_2(\mu\text{-}C_2)$ part to a $\mu\text{-}\eta^1{:}\eta^2$-acetylide coordination structure with an unsymmetrical $C_\alpha M_2$ triangle, resulting from π interaction between the C−C multiple bond and one of the two metal centers. Because back-donation from the dicationic $(\mu\text{-}PNNP^{Ph})Rh_2(CO)_2$ fragment is weaker than that from the monocationic $(\mu\text{-}PNNP^{Py})Rh_2(CO)_2$ fragment, the $\mu\text{-}\eta^1{:}\eta^2$-acetylide coordination features are less apparent for the $PNNP^{Ph}$ system. The Rh1···Rh2 (3.1967(2) Å) and Rh2···Rh2* separations (3.009(3) Å) are out of the range of bonding interactions, and the Rh2···Rh2* separation is shorter than that in **G** (3.173(2) Å). However, formation of the C_2-symmetrical structure of **12** in preference to the isomeric centrosymmetrical structure **12′** (Chart 1) suggests that there may be a weak bonding interaction between Rh2 and Rh2*, although the conformation may result from packing in the single crystal. Complex **12** should be formed via mechanisms analogous to those for **G**:[3b,d] i.e., desilylation of the $Me_3SiC{\equiv}C$

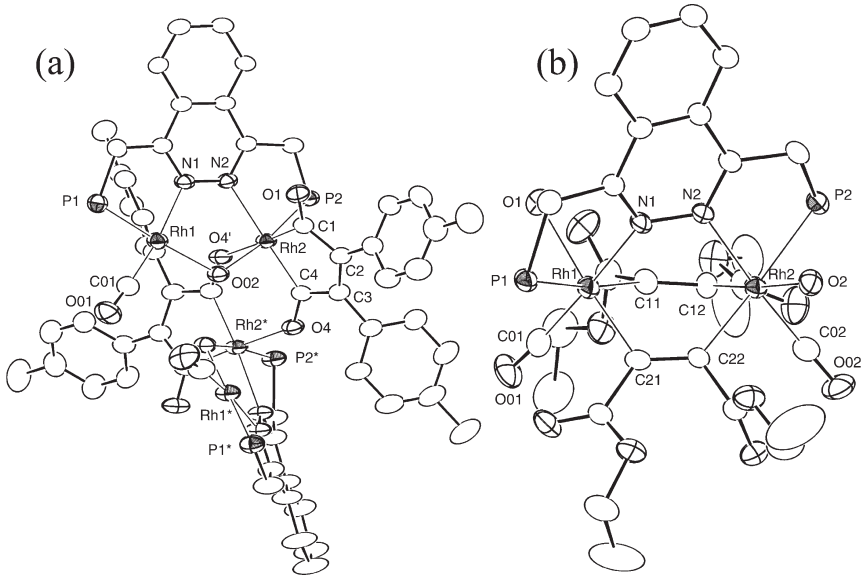

Figure 5. ORTEP views of the cationic parts of **13** (a) and **14** (b) with thermal ellipsoids at the 30% probability level. Phenyl groups are omitted for clarity.

Chart 1

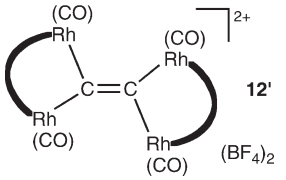

derivative of **11** followed by spontaneous deprotonation of the resultant μ_4-C_2H intermediate.

(iii). With Internal Alkyne. The $PNNP^{Ph}$ complex **7** reacted with internal alkynes to afford stable adducts with unique coordination structures (Scheme 5) in contrast to the $PNNP^{Py}$ system, giving unstable μ-η^2:η^2 adducts (Scheme 1).[3d]

Reaction of **7** with di-*p*-tolylacetylene in acetone gave the yellow product **13** in moderate yield. The ^{31}P NMR spectrum of **13**, containing a pair of doublet of multiplets signals,[9] suggests an unsymmetrical structure, and the dimeric structure has been characterized by X-ray crystallography (Figure 5a). The structure contains a 2,5-dioxorhodacyclopent-3-ene ring and a bridging hydroxo ligand, and coordination of the C═O group to the rhodium center in the other unit furnishes the cyclic, dimeric structure. The metallacycle results from oxidative metallacyclization of one molecule of the alkyne and two molecules of CO. As a result, one of the two rhodium centers (Rh2 included in the metallacycle) is a six-coordinate Rh(III) center, while Rh1 remains Rh(I). In accord with this change, the Rh−P/N distances associated with the Rh(III) center are slightly longer than those associated with the Rh(I) center (Rh1−P1 = 2.194(2) Å, Rh2−P2 = 2.241(2) Å; Rh1−N1 = 2.143(6) Å, Rh2−N2 = 2.226(5) Å). The *intraunit* Rh−Rh separation (3.5980(8) Å) is far beyond the range of bonding interactions.

Reaction of **7** with diethyl acetylenedicarboxylate, an alkyne molecule with electron-withdrawing substituents, afforded the totally different 1:2 adduct **14**, which was confirmed by X-ray crystallography (Figure 5b). Two molecules of the alkyne oxidatively add across the Rh−Rh linkage to form the bicyclic structure. In general, alkyne molecules with electron-releasing

Scheme 5

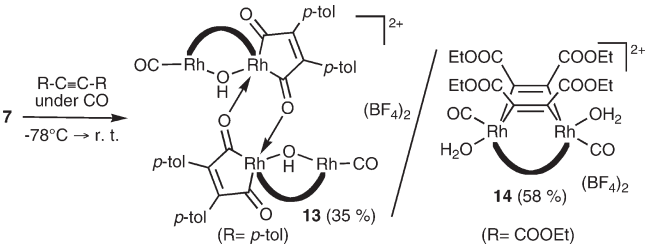

substituents couple with dinuclear species to form adducts with a tetrahedral M_2C_2 core, whereas those with electron-withdrawing substituents undergo insertion into the metal−metal bond.[16] A 1,4-dimetallacyclohexa-2,5-diene structure as in **14** has several precedents.[17] Coordination of water gives the six-coordinate structure.

Coordination Features of the $PNNP^{Ph}$ Ligand As Compared with Those of the $PNNP^{Py}$ Ligand. The following conclusion can be deduced from the obtained experimental results.

Many similarities in the structures of the reaction products of the carbonyl species **C** and **7** have been observed, not only for conventional species such as the dinuclear μ-acetylide complexes (**E** and **9**) but also for unique, tetranuclear μ_4-acetylide cluster compounds (**F** and **11**) and μ_4-dicarbide complexes (**G** and **12**). The present study reveals that the PNNP ligand set provides a scaffold for such unique structures, which have never been observed for other ligand systems.

Meanwhile, the following dissimilarities are also noted.

(1) Ring size effect. The enlarged six-membered ring in $PNNP^{Ph}$ causes shortening of the metal−metal distance, which frequently leads to *intraunit* M−M bond formation as exemplified by **6**.

(16) Hoffman, D. M.; Hoffmann, R.; Fisel, C. R. *J. Am. Chem. Soc.* **1982**, *104*, 3858.

(17) Clemens, J.; Green, M.; Kuo, C. M.; Fritchie, J. C., Jr.; Mague, T. J.; Stone, F. G. A. *Chem. Commun.* **1972**, 53. Smart, E. L.; Green, M.; Laguna, A.; Stone, F. G. A. *J. Chem. Soc., Dalton Trans.* **1977**, 1777. Jenkins, A. J.; Cowie, M. *Organometallics* **1992**, *11*, 2774.

(2) Charge effects. (i) Complexation of the neutral $PNNP^{Ph}$ ligand with cationic metal species provides more positively charged species, in which back-donation decreases when compared with the corresponding less positively charged $PNNP^{Py}$ analogues. The lesser number of CO ligands on the dinuclear carbonyl species **7** (vs **C**) should result from decreased back-donation to CO ligands (i.e., the Rh centers in **7** cannot support two CO ligands), and the less unsymmetrical μ-η^1:η^2 coordination structure in the μ_4-dicarbide complex **12** (vs **G**) arises from weaker back-donation from the dicationic $[(\mu\text{-}PNNP^{Ph})\{Rh(CO)_2\}_2]^{2+}$ moiety. (ii) More positively charged species are more Brønsted and Lewis acidic. For example, $Me_3SiC{\equiv}CH$ can be incorporated into both of the (μ-PNNP)Rh_2 systems but, in the case of the $PNNP^{Ph}$ system, subsequent desilylation and deprotonation leading to the μ_4-C_2 complex **12** occur spontaneously, owing to the enhanced electrophilicity at the Si center in the more Lewis acidic $PNNP^{Ph}$ derivative and the increased Brønsted acidity of the μ_4-C_2H moiety.

(3) Oxidative addition reactions (**13** and **14**). These are observed only for the $PNNP^{Ph}$ system.

Experimental Section

General Methods. All manipulations were carried out under an inert atmosphere by using standard Schlenk tube techniques. THF, ether, hexane (Na−K alloy), CH_2Cl_2 (P_2O_5), acetone (CaH_2), and ROH ($Mg(OR)_2$; R = Me, Et) were treated with appropriate drying agents, distilled, and stored under argon. ^1H and ^{31}P NMR spectra were recorded on a Bruker AC-200 instrument (^1H, 200 MHz; ^{31}P, 81 MHz; chemical shifts downfield from TMS (^1H) and H_3PO_4 (^{31}P)), and resonances and coupling constants are reported in ppm and in Hz, respectively. Solvents for NMR measurements containing 0.5% TMS were dried over molecular sieves, degassed, distilled under reduced pressure, and stored under Ar. IR and UV−vis−near-IR spectra were obtained on JASCO FT/IR 5300 and JASCO V-570 spectrometers, respectively. ESI-MS spectra were recorded on a ThermoQuest Finnigan LCQ Duo mass spectrometer. 1,4-Dichlorophthalazine[18] and $[M(cod)_2]BF_4$ (M = Rh, Ir)[2a] were prepared according to the published procedures. Other chemicals were purchased and used as received. Details of X-ray crystallography are included in the Supporting Information.

Ligand Synthesis (1). (i) Preparation of 2. To $O{=}PPh_3$ (28.3 g, 102 mmol) suspended in ether (80 mL) was added an ethereal solution of MeLi (1.0 M, 100 mL, 100 mol, 2.5 equiv) dropwise at room temperature, and the resultant mixture was stirred for 2 h to afford a brown solution.[5] To the mixture cooled to −78 °C was added dropwise a THF solution of 1,4-dichlorophthalazine (4.02 g, 20.2 mmol), and the mixture was stirred overnight. Then the reaction was quenched with water (500 mL) and the product was extracted with CH_2Cl_2 (1.2 L). Evaporation of the extract gave a yellowish solid, which was washed with toluene (100 mL) and then ether (50 mL). After drying under reduced pressure **2** was obtained as a colorless solid (6.78 g, 12.1 mmol, 60% yield). **2**: δ_H ($CDCl_3$) 8.41−8.36 (2H, m, phthalazine), 7.87−7.73 (10H, m, Ar), 7.44−7.35 (12H, m, Ar), 4.41 (4H, d, J = 14.0 Hz, CH_2P); δ_P ($CDCl_3$) 22.0; FAB-MS m/z 559 (M + H).

(ii) Preparation of 1. Addition of NEt_3 (5.1 g, 50 mmol) and $HSiCl_3$ (13.4 g, 99 mmol) to **2** (3.01 g, 5.39 mmol) suspended in toluene (300 mL) caused a rapid color change to yellow. Refluxing the mixture caused a change from a yellow suspension to a yellow solution. The mixture was cooled in an ice−water bath, and water (250 mL) and 20% aqueous NaOH (200 mL) were added. The product was extracted with CH_2Cl_2 (150 mL) and dried over $MgSO_4$. Evaporating the volatiles and washing with a mixture of CH_2Cl_2 (30 mL) and ether (45 mL) gave **1** as a colorless solid (1.45 g, 2.75 mmol, 51% yield). **1**: δ_H ($CDCl_3$) 8.23−8.18, 7.83−7.78 (2H × 2, m × 2, phthalazine), 7.54−7.46 (8H, m, Ph), 7.31−7.28 (12H, m, Ar), 4.10 (4H, s, CH_2P); δ_P ($CDCl_3$) −18.7. Anal. Calcd for $C_{34}H_{28}N_2P_2$: C, 77.36; H, 5.36; N, 5.32. Found: C, 77.04; H, 5.29; N, 5.21.

(iii) Preparation of Monosubstituted Ligand 3. A 1:1.5 reaction between $LiCH_2P(=O)Ph_2$ and 1,4-dichlorophthalazine as described for (i) was quenched just after the temperature of the mixture reached room temperature. Analogous workup and subsequent deoxygenation with $HSiCl_3/NEt_3$ gave **3** as a colorless solid (69% yield). **3**: δ_H ($CDCl_3$) 8.31−8.18, 8.00−7.88 (2H × 2, m × 2, Ar), 7.52−7.47 (4H, m, Ph), 7.30 (6H, m, Ph), 4.11 (2H, s, CH_2P); δ_P ($CDCl_3$) −18.2. Ligand **3** was converted to the Rh adduct [**3**·Rh(cod)]BF_4 by treatment with $[Rh(cod)_2]BF_4$ as described for **4a**, and the Rh adduct was characterized by X-ray crystallography (see the Supporting Information).

Preparation of COD Complexes, $[(\mu\text{-}PNNP^{Ph})\{M(cod)\}_2](BF_4)_2$ (4). (i) Rhodium Complex 4a (M = Rh). To a CH_2Cl_2 solution (15 mL) of $[Rh(cod)_2]BF_4$ (2.34 g, 5.76 mmol) was added **2** (1.45 g, 2.75 mmol) dissolved in CH_2Cl_2 (70 mL) over 1 h. After the mixture was stirred for 1 h at room temperature, the resultant red-brown solution was evaporated and the obtained residue was washed with a mixture of acetone (30 mL) and hexane (40 mL) three times to give **4a** (2.68 g, 2.39 mmol, 87% yield) as an orange powder. **4a**: δ_H ($CDCl_3$) 8.54−8.49, 8.25−8.20 (2H × 2, m × 2, phthalazine), 7.63−7.49 (20H, m, Ph), 5.15 (4H, d, J = 8.5 Hz, CH_2P), 4.04 (4H, br, =CH in cod), 2.48, 1.63 (8H × 2, br × 2, CH_2 in cod); δ_P 28.0 (d, J_{P-Rh} = 148.4 Hz); ESI-MS m/z 737 ($M^+ - 2\ BF_4$). Anal. Calcd for $C_{50.75}H_{53.5}B_2Cl_{1.5}F_8N_2P_2Rh_2$ (**4a**·0.75CH_2Cl_2): C, 51.39; H, 4.55; N, 2.36. Found: C, 51.47; H, 4.67; N, 2.38.

(ii) Iridium Complex 4b (M = Ir). Complex **1** (197.2 mg, 0.375 mmol) dissolved in CH_2Cl_2 (70 mL) was added to a CH_2Cl_2 solution (7 mL) of $[Rh(cod)_2]BF_4$ (376.9 mg, 0.76 mmol) over 1 h. After the mixture was stirred for 1 h at room temperature, the resultant deep red solution was evaporated. Dissolution of the obtained residue in hot EtOH (60 °C) followed by cooling to room temperature gave red crystals, which were collected by filtration and dried under reduced pressure. **4b** (309.0 mg, 0.238 mmol, 63% yield): δ_H ($CDCl_3$) 9.01−8.96, 8.52−8.48 (2H × 2, m × 2, phthalazine), 7.86 (8H, br, Ph), 7.63−7.59 (12H, m, Ph), 5.73 (4H, d, J = 8.5 Hz, CH_2P), 4.02 (4H, br, =CH in cod), 2.26, 1.80 (8H × 2, br × 2, CH_2 in cod); δ_P ($CDCl_3$) 24.1; ESI-MS m/z 827 ($M^+ - 2\ BF_4$). Anal. Calcd for $C_{51.5}H_{55}B_2Cl_3F_8N_2P_2Ir_2$ (**4a**·1.5CH_2Cl_2): C, 43.31; H, 3.88; N, 1.96. Found: C, 43.02; H, 3.78; N, 1.88.

Preparation of the μ-Cl Complex $[(\mu\text{-}PNNP^{Ph})\{Rh(CO)\}_2(\mu\text{-}Cl)]BF_4$ (5). CO was bubbled through a MeOH suspension (10 mL) of **4a** (121.4 mg, 0.0990 mmol) and NaCl (33.0 mg, 0.565 mmol) for 1 h. Addition of Et_2O (60 mL) gave a yellow precipitate, to which was added CH_2Cl_2 (15 mL) and water (15 mL). The organic layer was collected, dried over $MgSO_4$, and evaporated to afford **5** (71.7 mg, 0.0718 mmol, 73% yield) as a yellow powder. **5**: δ_H ($CDCl_3$) 8.52−8.48, 8.01−7.98 (2H × 2, m × 2, phthalazine), 7.88−7.78 (8H, m, Ph), 7.50−7.46 (12H, m, Ph), 4.82 (4H, d, J = 11.3 Hz, CH_2P); δ_P ($CDCl_3$) 57.1 (d, J_{P-Rh} = 168.3 Hz); IR (ν_{CO}) 2022 cm^{-1} (KBr). Anal. Calcd for $C_{36.25}H_{28.5}BCl_{1.5}F_4NPRh_2$ (**5**·0.25CH_2Cl_2): C, 46.72; H, 3.08; N, 3.01. Found: C, 46.73; H, 3.08; N, 3.01. Complex **5** was also obtained by carbonylation of **4a** in CH_2Cl_2, as described in the text.

Preparation of the Tetrarhodium Complex $[(\mu\text{-}PNNP^{Ph})_2\{Rh(CO)\}_4](BF_4)_2$ (6). A THF suspension (4 mL) of **4a** (51.8 mg, 0.0462 mmol) cooled to −78 °C was bubbled with CO for 30 min. After addition of $HSiEt_3$ (3.2 mg, 0.028 mmol) via a microsyringe the mixture was warmed to room temperature and further stirred for 1 h. Addition of hexane to the resultant black mixture gave black precipitates (**6**), which were collected by

(18) Amberg, W.; Bennani, Y. L.; Chada, R. K.; Crispino, G. A.; Davis, W. D.; Hartung, J.; Jeong, K.-S.; Ogino, Y.; Shibata, T.; Sharpless, K. B. *J. Org. Chem.* **1993**, *58*, 844.

filtration and dried under reduced pressure. **6** (33.7 mg, 0.020 mmol, 88% yield): δ_H (acetone-d_6) 8.88−8.83, 8.41−8.36 (4H × 2, m × 2, phthalazine), 7.82−7.44 (40H, m, Ph), 5.21 (8H, d, J = 9.8 Hz, CH_2P); δ_P (acetone-d_6) 49.6 (dq-like, J = 73 and 6 Hz);[9] IR (ν_{CO}) 1924 cm^{-1} (KBr), 1936 cm^{-1} (CH_2Cl_2); ESI-MS m/z 1663 ($M^+ - BF_4$), 1576 ($M^+ - 2\,BF_4$). Anal. Calcd for $C_{73.5}H_{58}B_2Cl_2F_8N_4P_4Rh_4$ (**6**·CH_2Cl_2): C, 47.77; H, 3.19; N, 3.05. Found: C, 47.48; H, 3.39; N, 3.08. Complex **6** was also obtained by carbonylation of **4a** in non-halogenated solvents such as THF and acetone, as described in the text.

Carbonylation of 4a in THF at −78 °C: Formation of [(μ-PNNP^{Ph}){(Rh(CO))}$_2$](BF$_4$)$_2$ (7). CO was bubbled through a THF suspension (4 mL) of **4a** (51.7 mg, 0.0461 mmol) cooled to −78 °C for 30 min. Addition of hexane to the resultant black mixture at −78 °C gave a yellow powder (**7**), which was collected by filtration and dried under reduced pressure. **7** (32.5 mg, 0.0338 mmol, 73% yield):[19b] δ_H (CD_3NO_2) 8.65−8.50, 8.45−8.41 (2H × 2, m × 2, phthalazine), 7.90−7.79 (8H, m, Ph), 7.72−7.60 (12H, m, Ph), 5.08 (4H, d, J = 10.4 Hz, CH_2P); δ_P (CD_3NO_2) 48.4 (m);[9] IR (ν_{CO}) 2008 cm^{-1} (KBr), 2098, 2078, 2045 cm^{-1} ($CDCl_3$ under CO).

Carbonylation of [(μ-PNNP^{Ph}){(Ir(cod))}$_2$](BF$_4$)$_2$ (4b) To Give [(μ-PNNP^{Ph})Ir$_2$(CO)$_5$](BF$_4$)$_2$ (8). CO was bubbled through an acetone solution of **4a** (29.8 mg, 0.0229 mmol) for 1 h. The solution immediately changed from red to yellow. After 1.5 h Et_2O (17 mL) was added under a CO atmosphere to precipitate the product, which was collected by filtration and dried under reduced pressure. **8** (22.3 mg, 0.0181 mmol, 79% yield): δ_H (acetone-d_6) 8.87−8.83, 8.47−8.42 (2H × 2, m × 2, phthalazine), 8.10−7.79 (8H, m, Ph), 7.72−7.50 (12H, m, Ph), 5.45 (4H, br, CH_2P); δ_P (acetone-d_6) 23.3 (m);[9] IR (ν_{CO}) 2085, 2023, 1751 cm^{-1} (KBr); ESI-MS m/z 995 ($M^+ - 2\,BF_4$), 967 ($M^+ - 2\,BF_4 - CO$). Anal. Calcd for $C_{39}H_{28}B_2F_4Ir_2N_2P_2$ (**8**): C, 38.25; H, 2.30; N, 2.29. Found: C, 38.38; H, 2.10; N, 2.50.

Preparation of Dirhodium μ-Acetylide Complex 9. CO was bubbled through a THF suspension (10 mL) of **4a** (200.5 mg, 0.179 mmol) cooled to −78 °C for 30 min. To the resultant solution of the carbonyl species **7** was added water (3.2 mg, 0.180 mmol) and *p*-tol-C≡CH (64.4 mg, 0.554 mmol), and then the mixture was warmed to room temperature. The solution color darkened. Stirring the mixture for 1 h caused precipitation of an orange solid, which was collected and washed with THF (2 mL × 3) to afford **9** after drying under reduced pressure. **9** (110.7 mg, 0.102 mmol, 57%): δ_H (acetone-d_6) 8.80−8.75, 8.39−8.34 (2H × 2, m × 2, phthalazine), 7.97−7.87 (8H, m, Ph), 7.78 (2H, d, J = 8.0 Hz, tol), 7.59−7.55 (12H, m, Ph), 7.22 (2H, d, J = 8.0 Hz, tol), 5.26 (4H, d, J_{HP} = 10.6 Hz, CH_2P), 2.36 (3H, s, Me in tol); δ_P (acetone-d_6) 59.6 ($^1J_{PRh}$ = 139.0 Hz, $^1J_{RhRh'}$ = 2.5 Hz, $^2J_{PRh'}$ = 0.8 Hz);[9] IR (ν_{CO}) 2003 cm^{-1} (KBr); ESI-MS m/z 903 ($M^+ - 2\,BF_4$), 967 ($M^+ - 2\,BF_4 - CO$). Anal. Calcd for $C_{46}H_{37}BCl_2F_4N_2O_2P_2Rh_2$ (**9**·CH_2Cl_2): C, 51.77; H, 3.85; N, 2.67. Found: C, 51.38; H, 3.47; N, 2.61.

Formation of Tetrarhodium Diacetylide Cluster Compound 10. When an acetone solution of **9** was stirred under an N_2 atmosphere for 24 h at room temperature, the solution darkened. Addition of hexane caused precipitation of **10** (68% yield), which was collected and dried under reduced pressure. **10**:[19a] δ_H (CD_3NO_2) 8.63−8.22, 7.97−7.12 (m, aromatic), 6.05, 5.37 (2H × 2, d × 2, J = 8.2 Hz, C_6H_4 in *p*-tol), 1.76 (3H, s, Me in tol).[20]

Preparation of Tetrarhodium Monoacetylide Cluster Compound 11. CO was bubbled through a THF suspension (4 mL) of a mixture of **9** (26.3 mg, 0.0266 mmol) and **4a** (29.8 mg, 0.0266 mmol) cooled to −78 °C for 1 h. Then the mixture was wormed to room temperature and further stirred for 1.5 h to give a black precipitate, which was collected and dried under reduced pressure. **11** (43.5 mg, 0.0223 mmol, 84% yield):[19a] δ_H (CD_2Cl_2) 8.40−8.35 (2H, m, phthalazine), 8.23 (2H, d, J = 8.0 Hz, tol), 8.08−8.04 (4H, m, phthalazine), 7.63−7.30 (42H, m, Ph and tol), 7.78 (2H, d, J = 8.0 Hz, tol), 4.85 (8H, d, J_{HP} = 11.2 Hz, CH_2P), 2.55 (3H, s, Me in tol); δ_P (CD_2Cl_2) 58.6 (d, J_{PRh} = 160.0 Hz); IR (ν_{CO}) 2005 cm^{-1} (KBr); ESI-MS m/z 903 ($M^+ - 2\,BF_4 - 2\,CO$).

Preparation of Tetrarhodium Dicarbide Cluster Compound 12. A THF solution of **7** (5 mL) was generated from **5a** (96.5 mg, 0.0860 mmol) at −78 °C as described for **9**. After addition of $Me_3SiC{\equiv}CH$ (50.7 mg, 0.516 mmol) the mixture was warmed to room temperature and stirred for 1.5 h. The resultant black precipitate **12** was collected and washed with acetone (3 mL). **12** (42.7 mg, 0.0241 mmol, 60% yield): δ_H (CD_3CN) 8.36−8.29 (8H, m, phthalazine), 7.63−7.29 (40H, m, Ph and tol), 4.55 (8H, d, J_{HP} = 10.6 Hz, CH_2P); δ_P (CD_3CN) 57.2 (d, J_{PRh} = 144.1 Hz); IR (ν_{CO}) 2006 cm^{-1} (KBr); ESI-MS: m/z 1687 ($M^+ - BF_4$), 801 ($M^+ - 2\,BF_4$; dication). Anal. Calcd for $C_{72}H_{56}B_2F_8N_4O_4P_4Rh_4$ (**12**): C, 49.41; H, 3.22; N, 3.20. Found: C, 49.70; H, 3.47; N, 3.31.

Reaction of 7 with Di-*p*-tolylacetylene To Give 13. A THF solution of **7** (5 mL) was generated from **5a** (96.6 mg, 0.0861 mmol) at −78 °C as described for **9**. To the resultant solution was added di-*p*-tolylacetylene (53.3 mg, 0.258 mmol) dissolved in acetone (2 mL), and the mixture was gradually warmed to room temperature and stirred for 2 h to give a dark brown solution. Addition of hexane (30 mL) formed a precipitate, which was collected and dried under reduced pressure. Recrystallization from acetone (3 mL)−Et_2O (1 mL) gave **13** as a yellow powder (34.0 mg, 0.0151 mmol, 35% yield). **13**:[19a] δ_H (CD_3CN) 8.70−8.66, 8.54−8.51, 8.36−8.21, 7.83−7.71, 7.53−7.41, 7.05−6.97 (aromatic), 6.65 (8H, d, J = 7.9 Hz, tol), 5.15−4.75 (8H, m, CH_2P), 2.26, 2.25 (3H × 2, s × 2, Me in tol); δ_P (CD_3CN) 53.5 (dd, $^1J_{PRh}$ = 146.2 Hz, $^3J_{PRh}$ = 3.2 Hz), 36.4 (dd, $^1J_{PRh}$ = 157.3 Hz, $^3J_{PRh}$ = 3.2 Hz); IR (ν_{CO}) 1992, 1638 cm^{-1} (KBr); ESI-MS m/z 1039 ($M^+ - 2\,BF_4$; dication).

Reaction of 7 with Diethyl Acetylenedicarboxylate To Give 14. The reaction was carried out as described for **13** using **5a** (72.0 mg, 0.0539 mmol) and diethyl acetylenedicarboxylate (96.1 mg, 0.565 mmol). After the mixture was stirred for 2 h, a yellow precipitate appeared, were collected, which was washed with THF (2 mL) and dried under reduced pressure. **14** (yellow powder, 72.0 mg, 0.0539 mmol, 58% yield):[19a] δ_H (CD_3CN) 8.67−8.62, 8.45−8.40, 8.36−8.27, 7.90−7.87, 7.44−7.08 (aromatic), 5.40 (2H, dd, J_{HH} = 18.5 Hz, J_{HP} = 12.5 Hz, CH_2P), 5.09 (2H, dd, J_{HH} = 18.5 Hz, J_{HP} = 5.5 Hz, CH_2P), 4.08−3.92 (4H, m, Et), 3.74−3.64, 3.43−3.31 (2H × 2, m × 2, Et), 1.21−1.13, 0.87−0.80 (6H × 2, Et); δ_P (CD_3CN) 22.1 (d, J = 73.7 Hz); IR (ν_{CO}) 2085, 1677 cm^{-1} (KBr); ESI-MS m/z 1145 ($M^+ - 2\,BF_4$; dication).

Acknowledgment. We are grateful to the Ministry of Education, Culture, Sports, Science and Technology of the Japanese Government and the Japan Society for Promotion of Science and Technology for financial support of this research (Grants-in-Aid for Scientific Research Nos. 18065009, 20044007, and 22350026).

Supporting Information Available: Text, tables, figures, and CIF files giving crystallographic data and additional characterization data. This material is available free of charge via the Internet at http://pubs.acs.org.

(19) (a) An analytically pure sample could not be obtained despite several attempts, presumably because of tarry impurities. (b) An analytically pure sample could not be obtained because of the instability.

(20) A ^{31}P NMR signal and the ^1H NMR signals for the CH_2P part could not be located, presumably owing to some fluxional process. VT analysis was hindered by the lower solubility of **10** in organic solvents and the higher melting point of CD_3NO_2 (Figure S12, Supporting Information).